

Off-Plane X-ray Grating Spectrometer for the International X-ray Observatory

Randall L. McEntaffer*¹, Neil J. Murray², Andrew Holland², Chuck Lillie³, Suzanne Casement³,
Dean Dailey³, Tim Johnson³, Webster Cash⁴, Phil Oakley⁴

¹University of Iowa, Department of Physics and Astronomy, Van Allen Hall, Iowa City, IA

²Open University, Planetary and Space Sciences Research Institute, Milton Keynes, UK

³Northrop Grumman Aerospace Systems, Redondo Beach, CA

⁴University of Colorado, Center for Astrophysics and Space Astronomy, Boulder, CO

ABSTRACT

A dispersive spectrometer onboard the International X-ray Observatory (*IXO*) provides a method for high throughput and high spectral resolution at X-ray energies below 1 keV. An off-plane reflection grating array maximizes these capabilities. We present here a mature mechanical design that places the grating array on the spacecraft avionics bus 13.5 m away from the focal plane.

Keywords: spectroscopy, diffraction gratings, CCDs, International X-ray Observatory

1. INTRODUCTION

The International X-ray Observatory (*IXO*) is a new X-ray telescope that has its roots in the technology development accomplished by the former Constellation-X mission concept and XEUS mission concept. As such, this observatory is a collaborative effort involving NASA, ESA and JAXA. The fundamental astrophysics that will be addressed by *IXO* include the local environment of black holes, the formation of supermassive black holes, large scale structure in the Universe, and the processes that tie these together. These science goals drive the performance requirements for the telescope and instruments onboard *IXO*. The telescope will provide 3 m² of effective area at 1.25 keV with 5 arcsec (half power diameter) angular resolution. Instruments include a Wide Field Imager (WFI), a Hard X-ray Imager (HXI), a High Time Resolution Spectrometer (HTRS), an X-ray Polarimeter (XPOL), an X-ray Microcalorimeter Spectrometer (XMS) and an X-ray Grating Spectrometer (XGS). The WFI is an imaging spectrometer with an 18 × 18 arcmin field of view and moderate spectral resolution from 0.1–15 keV. The HXI operates simultaneously with the WFI and extends the energy range to 40 keV over a 12 arcmin field. The HTRS provides timing measurements of bright X-ray sources, up to 10⁶ counts per second over the 0.3–10 keV band. Polarization levels as low as 1% will be measured by XPOL for sources with 1 mCrab of flux over the 2–6 keV band. The two high spectral resolution instruments are the XMS and the XGS. The XMS is a non-dispersive imaging spectrometer that can provide 2.5 eV of energy resolution from 0.3–7.0 keV over a 2 × 2 arcmin field of view. However, given its constant energy bins, the XMS cannot achieve the spectral resolution performance requirements at the softest X-ray energies. This requirement is a spectral resolution of 3000 ($\lambda/\Delta\lambda$) from 0.3–1.0 keV. To achieve this, *IXO* must incorporate a dispersive grating spectrometer, the XGS. The reference design for the XGS places an array of gratings in the covering beam of the telescope. The gratings intercept the light and disperse onto an array of CCDs at the focal plane. Two options are being considered for the XGS. One of these utilizes Critical Angle Transmission (CAT) gratings while the other utilizes off-plane reflection gratings. This paper will discuss the implementation of the latter in an Off-Plane X-ray Grating Spectrometer (OP-XGS).

*randall-mcentaffer@uiowa.edu; phone (319) 335-3007; fax (319) 335-1753

2. OFF-PLANE X-RAY GRATING SPECTROMETER (OP-XGS)

2.1 Introduction

The purpose of the OP-XGS is to provide high spectral resolution ($\lambda/\Delta\lambda > 3000$) at low energies (0.3-1.0 keV) as a complement to the X-ray Microcalorimeter Spectrometer (XMS). The spectrometer consists of an array of reflection gratings in the off-plane mount¹, that diffracts light onto an array of dedicated CCDs. Light intersects the surface of the grating at grazing incidence, 2.7° , and nearly parallel to the groove direction. This maximizes the illumination efficiency on the gratings. Furthermore, the groove profile can be blazed to preferentially diffract light to only one side of zero order thus increasing the efficiency further. The blaze angle is chosen to maximize efficiency around 35 \AA in first order (1 keV efficiency peaks in 3rd order) and is set to 12° . The off-plane geometry leads to diffraction along an arc at the focal plane. A summary of the generic off-plane geometry is shown in Figure 1.

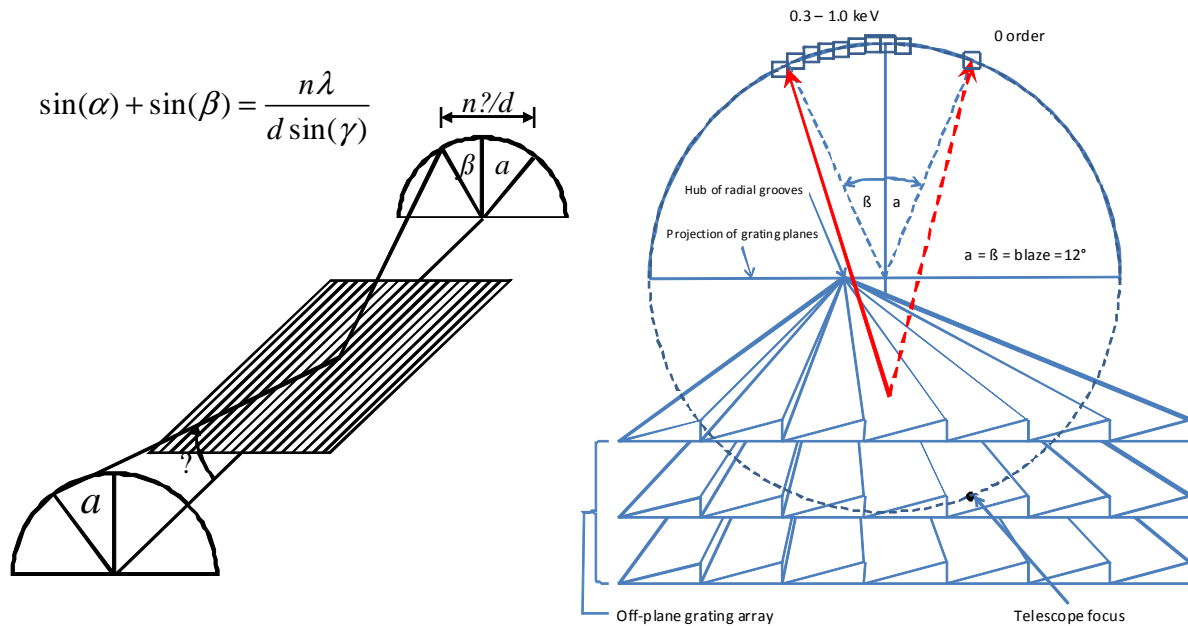


Figure 1: On the left an incoming ray of light intersects a grating in the off-plane mount with an azimuthal angle of α and graze angle of γ . Light is diffracted to an angle of β , dependent on wavelength and according to the grating equation. The diagram to the right shows the arc of diffraction at the focal plane and depicts several off-plane gratings placed in an array in order to collect light from some fraction of a telescope beam.

The viewing orientation for the diagram on the right is normal to the focal plane. Therefore, we are looking approximately down the optical axis. In this orientation the gratings are extending from the focal plane toward the observer. In reality, the gratings will not extend from their position in the spacecraft all the way to the focal plane, but this situation is shown here for illustrative purposes. The large arrows show two possible paths for a ray of light intersected by a grating. If the light was allowed to continue unimpeded by gratings, then it would propagate to the telescope focus which happens to lie in the grating focal plane along the circle defined by the arc of diffraction. The dashed arrow shows specular reflection into zero order, which lies vertically displaced from the telescope focus, while the solid arrow depicts a diffracted beam on one side of zero order.

This diagram illustrates several of the key concepts that will be utilized for IXO. First, given the shallow graze angle necessary for efficient reflection of X-rays, multiple gratings will need to be placed into an array to capture the appropriate section of the telescope beam and ultimately achieve the required effective area. A small, representative section is shown in Figure 1. Second, this figure demonstrates the concept of blazing the grating grooves to maximize efficiency in only plus or minus orders². Third, the grating grooves will also exhibit a radial profile as opposed to typical parallel grooves³. In order to maintain a constant graze angle over the array, the gratings are fanned such that the radial grooves of all gratings converge to a point on the focal plane denoted as the hub. This radial profile will match the convergence of the telescope beam which will maintain a consistent α over the array, thus nullifying any aberrations caused by the gratings. Therefore, the spectral resolution obtained by the gratings will be limited by the quality of the telescope. Spectral lines will be approximately Gaussian with a FWHM equal to the half power diameter (HPD) of the telescope point spread function (PSF). However, the effective telescope PSF can be minimized by only sampling a fraction of the beam. Limiting the azimuthal coverage of the grating array, or “subaperturing”, will decrease the FWHM of the spectral lines, thus increasing spectral resolution³.

The high illumination efficiency combined with the use of a blazed grating ensure high throughput in diffracted orders. Furthermore, the use of radial profiles and the technique of subaperturing will maximize spectral resolution. In this way the OP-XGS can easily meet the requirements for IXO (Table 1).

Spectral Resolution	$\lambda/\Delta\lambda > 3000$ over bandpass
Effective Area	$> 1000 \text{ cm}^2$ over bandpass
Bandpass	0.3 – 1.0 keV

Table 1: IXO OP-XGS performance requirements

2.2 OP-XGS configuration

An off-plane grating array can achieve the instrument performance requirements at any position along the optical axis from just aft of the optics to just 3 m away from the focal plane. However, due to CCD accommodation at the focal plane along with mass considerations, it was determined that a convenient position to place the grating array would be at the spacecraft avionics bus which is located ~6.5 m downstream from the optics. This places the grating array 13.5 m away from its focal plane. Figure 2 shows the placement of the grating array relative to the rest of the spacecraft. The telescope beam enters the grating array with a graze angle of 2.7° and is then reflected away from the telescope focus onto an array of CCDs. The array is mounted to the forward side of the avionics bus facing the optics. The placement is independent on azimuth, but was chosen to conveniently place the CCD camera on the Fixed Instrument Platform (FIP). A close-up of this position is shown in Figure 3. As seen in Figure 1, the CCDs lie along the arc of diffraction. Therefore, the CCD camera box is oriented orthogonal to the radial direction. Some CCD electronics are located in the camera head but an external CCD electronics box will also be required.

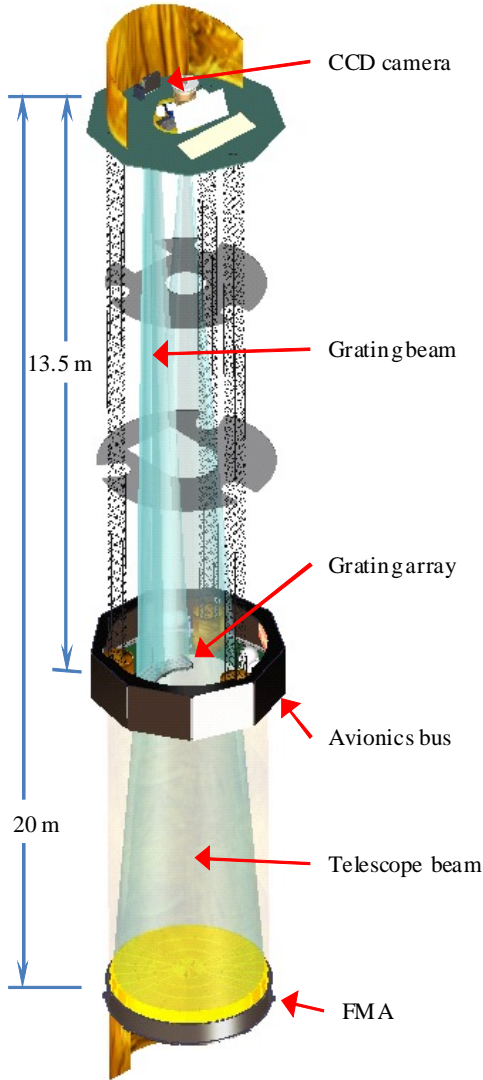


Figure 2: Grating array position relative to the spacecraft. Placing the gratings at the avionics bus results in a separation of 13.5 m from the focus.

Figure 4 takes a closer look at the grating array mounted to the spacecraft bus. The array is mounted to the forward side of the bus, the side facing the optics. In this way it is free from any interference with avionics equipment, electronics or the deployable masts. There is ample room for the structure in addition to flexible heaters and temperature sensors which stabilize the temperature of the gratings around room temperature. The heater controller box is mounted in proximity to the grating array to minimize mass and cabling required.

Figure 5 details the individual components of the grating array. The most basic component of the array is an individual grating. Each grating will have a blazed (at 12°), radial groove profile that matches the convergence of the telescope beam. A groove density of 5500 grooves/mm is adequate to achieve the spectral resolution requirements and is currently well

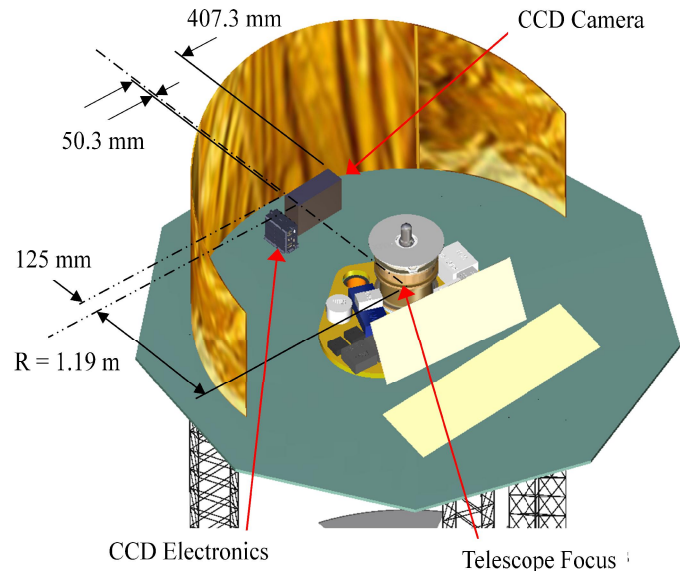


Figure 3: CCD position on the FIP. Approximate size of the camera and position relative to the telescope focus are given.

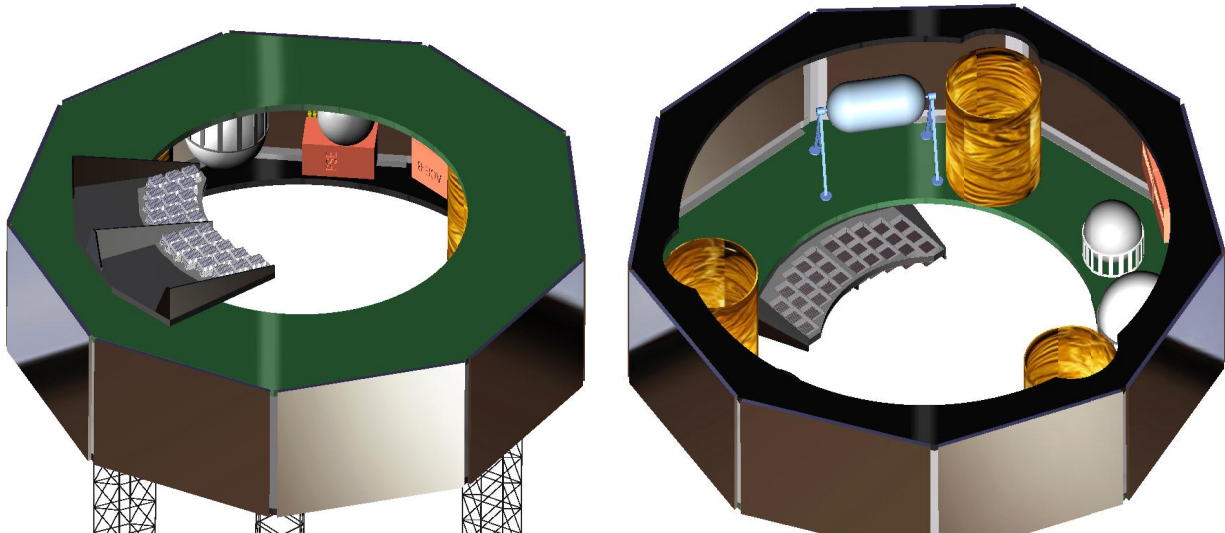


Figure 4: Placement of the grating array on the avionics bus. On the left the array is mounted on the forward side of the bus, facing the optics. The deployable masts are visibly protruding from the other side. The figure on the left shows the underside of the bus which houses the avionics and deployable mast mounts.

within the state of the art in grating manufacturing. We will also study the effect of going to higher densities and therefore higher dispersion both from the technical and scientific perspectives to optimize the science return for minimal technical risk. The reflective face of the grating, which is grooved, measures $100 \text{ mm} \times 100 \text{ mm}$. The body or “substrate” of the grating changes in thickness, starting at 2 mm on one edge, increasing to 4 mm at the center and then thinning back down to 2 mm at the opposite edge to form a trapezoidal profile as evident in model on the left side Figure 5. This viewing orientation looks at the back of the grating. The reflective surface is on the opposite side and contains the grooves which run approximately vertical. Trapezoidal substrates allow for tighter packing in a module and increased throughput. This trapezoidal substrate is then light-weighted to provide mass savings without overly decreasing the structural integrity of the substrates. The current packing of the modules leads to a mechanical

throughput of 70%. However, this number may be increased through additional light-weighting. This will be studied in the future, but is not critical in achieving the requirements.

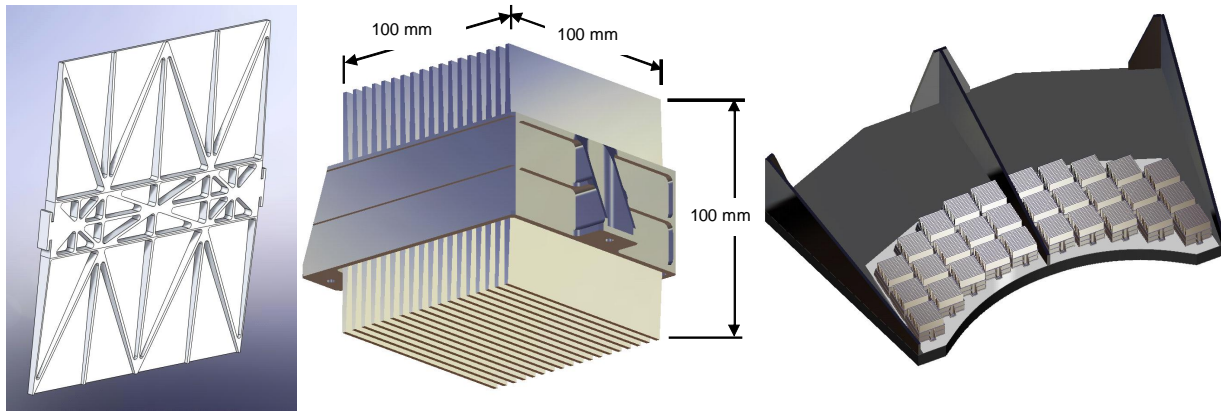


Figure 5: The backside of an individual grating is shown on the left. The structure has been light-weighted to reduce mass. The tabs on the side, near the middle, are used to mount each grating into a module as shown in the center. Each module houses 18 gratings. 30 modules are then co-aligned into an array as shown on the right. The modules utilize three mount points for adjustment in tip, tilt and piston.

The next component in Figure 5 is a grating module⁴. Each module holds 18 gratings. The tabs on the side of the grating, which are evident on the left of the figure, epoxy into a groove on the interior surface of the module structure. Mounting the gratings in this way minimizes mechanical effects of the module mount on the grating surface such as the transmission of mechanical and thermal stresses. The gratings are not parallel to one another. Given that an individual module intersects a range of angles from the converging telescope beam, the gratings are fanned over a small range of angles to maintain the 2.7° graze over the extent of the module and ultimately the array. 30 of these modules are co-aligned into an array as shown on the right of the figure. Each module has three mount points to adjustment tip, tilt and piston for alignment. The main body of the grating array structure which mounts to the avionics bus is constructed from Glass Fiber Reinforced Polymer (GFRP) facesheet with an aluminum honeycomb. A titanium frame is bonded to this main body using a fiberglass CTE buffer layer and mechanically captured. The modules then mount to this titanium frame. It is important to note that the module and array structures shown here are capable of achieving the performance requirements with modest weight and little obscuration. However, we will study methods for further optimization of the structure to decrease mass and obscuration.

2.3 OP-XGS CCD array

A representative CCD for the OP-XGS CCD array is shown in Figure 6. These CCDs measure 30 mm in the dispersion direction and 15 mm in the cross-dispersion direction. To increase the frame rate of the CCDs the pixels will measure 15 μm in the dispersion direction and 100 μm in the cross-dispersion direction. While operating in the typical frame transfer mode, the entire image area is integrated and then rapidly transferred into the store section for readout. The readout will occur through 4 parallel output nodes per CCD. Integration times will be determined by the science target, but will also factor in the necessary brightness of the zero order image (λ calibration) and characterization of stray-light. The maximum frame rate achieved will be 32 Hz with a noise equivalent signal of ≤ 8 electrons rms.

The 13.5 m distance between the gratings and the CCD array combined with a groove density of 5500 grooves/mm leads to a dispersion of 0.13 \AA/mm . Therefore, this dispersion along with the required first order wavelength band of 12–41 \AA results in a CCD array utilizing 9 CCDs that measure 30 mm in the dispersion direction. Of these 9 CCDs, one will monitor zero order while the other 8 capture dispersed light. Figure 7 displays the array of 9 CCDs along with dimensions and positions of various first order wavelengths of light along the arc of diffraction. The vertical lines

depicting the position of first order wavelengths in no way mimic the true point spread function of the spectral lines, but are shown merely for reference.

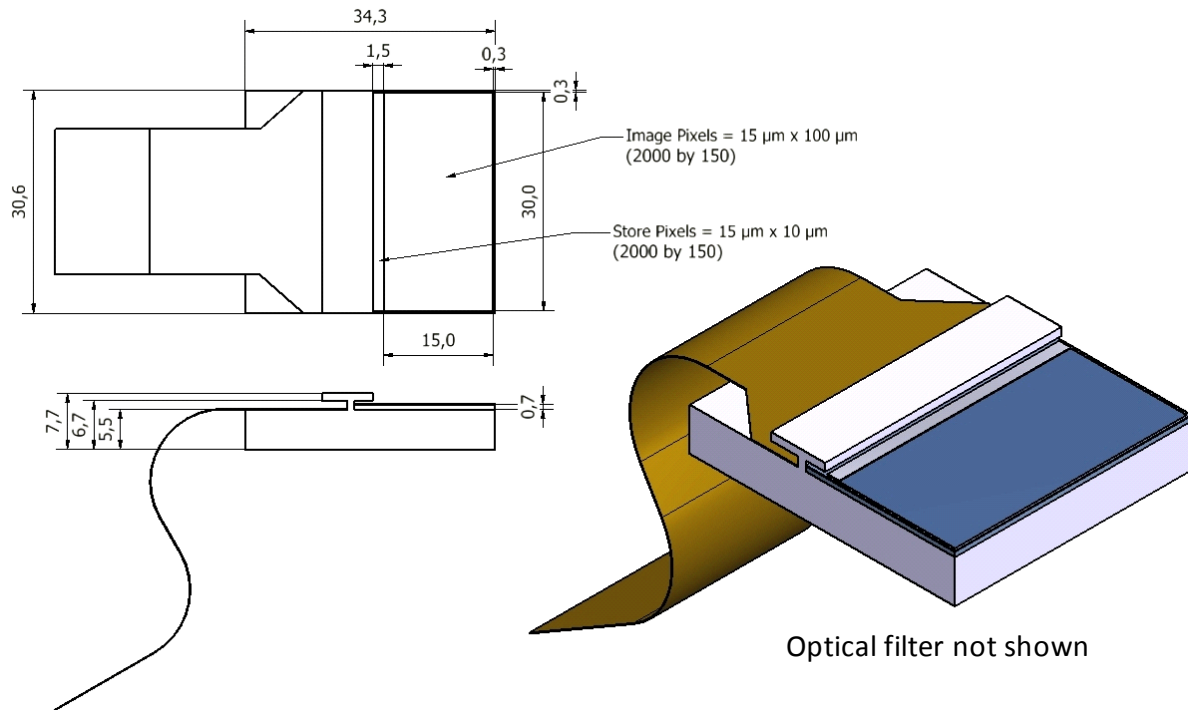


Figure 6: Dimensions of a single CCD

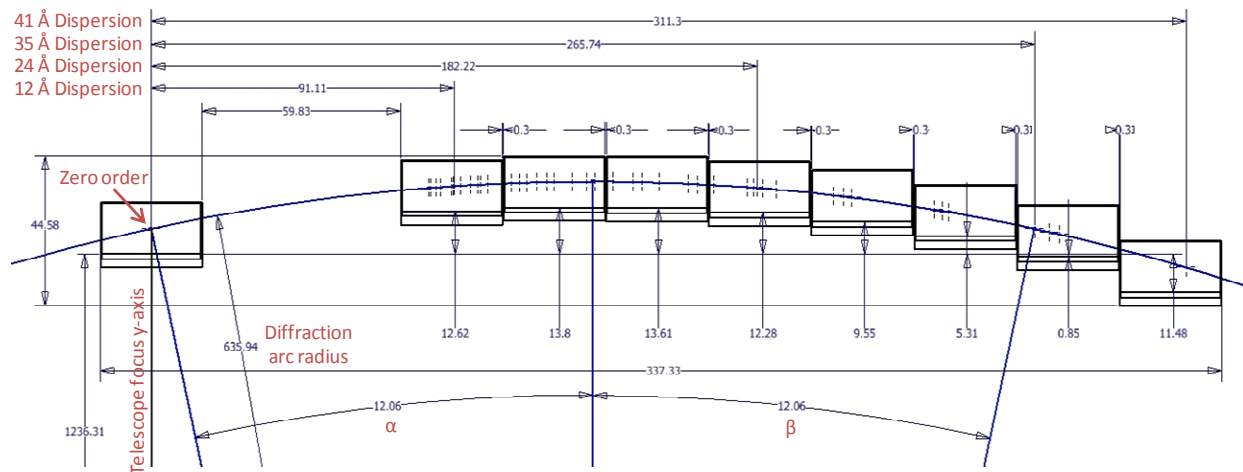


Figure 7: Dimensioned drawing of the CCD array with dimensions in mm. The arc of diffraction with corresponding wavelength positions are shown for reference. The vertical lines do not duplicate the actual spectral line PSF.

To limit the amount of noise due to unwanted or stray light, the CCDs will incorporate an optical blocking filter. The optical blocking filter has high TRL from XMM which can be used as a baseline⁵, and comprises a 26 nm layer of MgF_2 and a 45-75 nm layer of Al deposited directly on the CCD giving a reduction in stray light between 10^2 – 10^5 . We anticipate making refinements to the XMM-type filter, so here assume the thinnest XMM filter as the baseline for performance estimation purposes, which is consistent with the $>100\times$ frame rate over the XMM RGS. The expected

attenuation of soft X-rays due to the optical blocking filter is shown in Figure 8. We choose this layer since it maximizes the 200-400 eV transmission which will enhance the soft X-ray science.

Another component of the OP-XGS CCD array is the radiation shielding. Radiation shielding around the detectors protects the CCDs from the environmental hazards of the L2 orbit including solar wind particles and high energy photons. Such hazards not only cause spurious events, but are responsible for more serious side effects such as damage to the CCDs, an increase in the noise level, and a decrease in charge transfer efficiency. Therefore, a large fraction of the CCD assembly mass (37%) can exist in this shielding. Future studies include accurate characterization of the L2 radiation environment that *IXO* will encounter and optimization of the shielding given these findings. Furthermore, a detailed study will be preformed to characterize the effects of radiation damage to the CCDs to determine a maximum operating temperature for an acceptable level of charge transfer efficiency. This will determine whether charge injection strategies will be required and to what level.

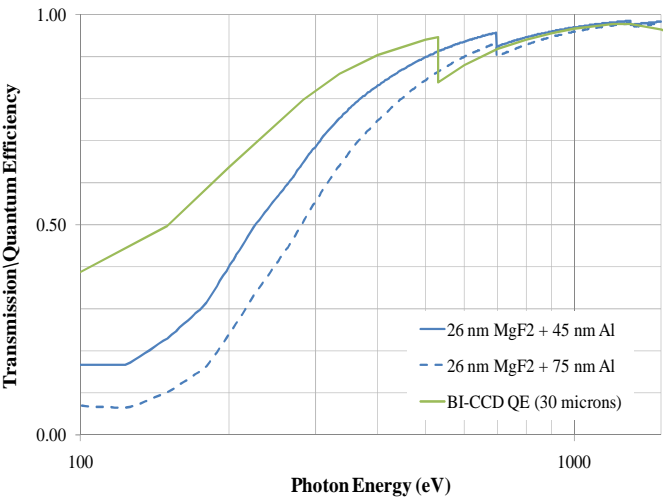


Figure 8: Soft X-ray transmission through the optical blocking filter comprised of 26 nm MgF₂ plus 45 nm Al and the modeled quantum efficiency of a 30 μm, back-illuminated CCD.

The CCD array electronics will consist of three main subsystems: the Proximity Electronics, the Drive Electronics and the Digital Processing Electronics. The Proximity Electronics will consist of filters and pre-amps for the signals as well as Correlated Double Sampling (CDS) Application Specific Integrated Circuits (ASICs), incorporating ADCs. These ASICs will be close-coupled, low noise, and multi-channel given the 4 output nodes per CCD. These Proximity Electronics are placed adjacent to the CCDs and therefore reside inside the CCD camera enclosure. The Drive Electronics consist of a housekeeping card, a thermal control card, a clock, and bias generators. These cards will be contained within a separate enclosure. The final enclosure will house the Digital Processing Electronics which consist of a bus interface card, a camera control card, a command card, and the discriminator. The power requirements for these components⁶ are listed in Table 2. Furthermore, a block diagram showing the relationship between the various components of the CCD electronics is displayed in figure 9. Simply stated, photons are counted by the CCDs as a charge pulse at a certain position which is then passed into the proximity electronics ASICs. These then pass the digital signal on to the Digital Processing Electronics where the counts are reduced into a relevant signal for telemetry. Meanwhile, a camera control card is controlling the clocking and biasing of the CCD as well as a thermal control card which is monitoring and maintaining CCD temperatures.

CCD Component	Unit Power (W)	CCD Component	Unit Power (W)
Pre-amps	2.5	Housekeeping	2
ASICs	2.5	Bus Interface	4
Thermal Control	15	Camera Control	4
CCDs	3	Discriminator	10
ADCs	2.5	Signal processors	2.5
Total		48	

Table 2: OP-XGS CCD electronics power budget

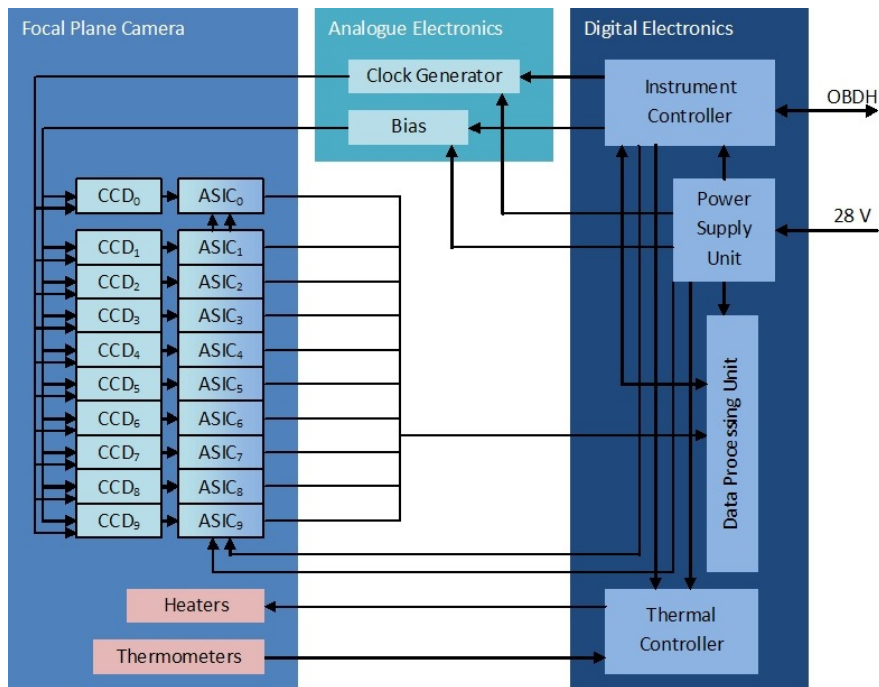


Figure 9: OP-XGS CCD camera electrical block diagram.

CCD₅ and CCD₉. The PRT data will be used by the Thermal Controller to ensure a homogenous heat distribution throughout the array. Four heater elements are required on the focal plane camera to regulate the operating temperature of the CCDs. This is a redundant system given two heaters on two circuits. These will be located on the rear surface of the cold bench, below CCD₀, CCD₁, CCD₅ and CCD₉.

Finally, the CCDs in the detector array must be cooled sufficiently to suppress the leakage (dark) current and mitigate in-flight radiation damage. The CCDs will have a maximum operating temperature of -90°C and minimum of -120°C , stabilized to $\pm 0.2^{\circ}\text{C}$ during operation. This level of control is routinely accomplished for space based detectors. The CCDs will be affixed to a bench that has a thermal link to a passive radiator. Heaters and platinum resistance thermometers (PRTs) in a feedback loop will be used to control the operating temperature of the array. Figure 10 shows the thermal control schematic for the CCD array. The array will have 8 PRTs, located on the focal plane camera above and below CCD₀, CCD₁,

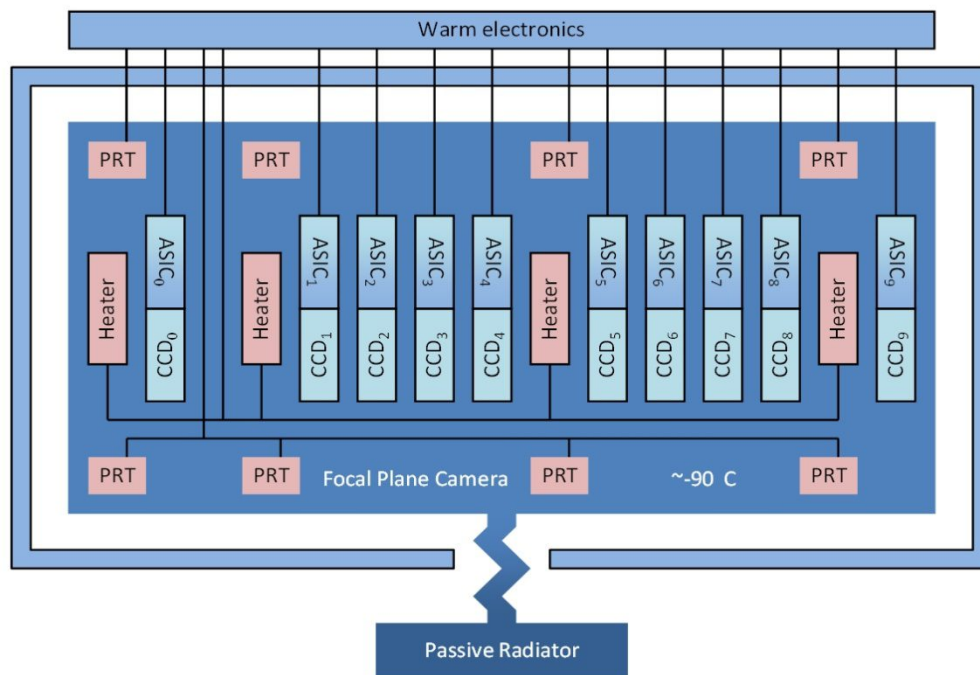


Figure 10: Thermal control schematic for the CCD camera.

2.4 OP-XGS grating array thermal control

The spectral resolution of the OP-XGS depends on several factors including the optical quality of the surface of the gratings. Of the six degrees of freedom, grating pitch drives the tolerances. Grating pitch is rotation about an axis that is in the plane of the grating surface but orthogonal to the groove direction. This leads to a requirement of a $\sim\lambda/4$ surface along the groove direction (measured at 6563 Å). This surface quality can be obtained using current machine tolerances. However, it must be maintained during flight. Deformation due to thermal excursions easily dominates the sources for surface manipulation during flight. This leads to a requirement of ± 0.5 K thermal gradient along the groove direction (2.7° off of the telescope optical axis) in order to maintain flatness over the gratings in the pitch direction. In order to monitor and control temperature of the grating array, a thermal control unit measuring approximately 23 x 30 x 8 cm with 3 electronics boards must be accommodated in the spacecraft nearby. Proximity is desired due to the potentially large number of heaters and temperature sensors that will need to be controlled and generate a significant amount of harness. A CAD model showing the placement of the thermal control unit within the spacecraft bus is shown on the left side of Figure 11.

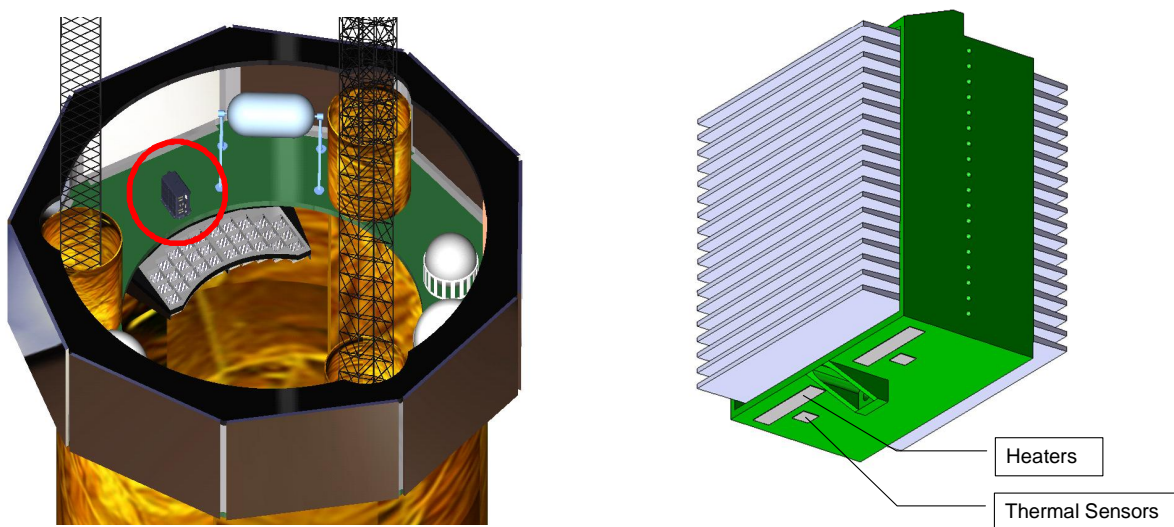


Figure 11: An engineering model showing the placement of the grating array thermal control box is displayed on the left. The box is highlighted with a red circle. On the right is an engineering model of a module of gratings showing the position of 2 of the 4 heaters and temperature sensors for each of the modules.

To minimize alignment errors during operations, the XGS grating array will be held at the same temperature in flight as during assembly and alignment, i.e. 23°C . This is necessary because the thin gratings will be made of a structural material, Beryllium, which has a moderate coefficient of thermal expansion. The grating modules are assumed to be cold in the absence of heaters due to the thermal balance of the spacecraft. Thus the OP-XGS gratings will be heated to the required temperature of $23\pm 0.5^\circ\text{C}$. The sizing of these heaters will be dependent on the overall system thermal design. Under survival and safe mode conditions, grating temperature only has to be maintained within -20 to $+40^\circ\text{C}$. Thermal design trade studies will be performed to determine the optimum method of heating based on optical-thermal requirements. The optical-thermal requirements will be based on the allowable radial and axial gradients and absolute temperature differences from 23°C required to maintain optical alignment and performance. Beryllium was selected for the gratings for its high specific stiffness, but also has high thermal conductivity, which will aid in minimizing thermal gradients. We have baselined using Minco polyimide flexible heaters configured to provide sufficient heating without being too large for mounting. For example, the Minco model HK5568R13.1 can provide up to 2W of heating at 5V in a package that is 0.25 x 1 inch (6.3 x 25 mm) for each. The reference design uses 4 of these heaters per grating module (120 total) as shown on the right side of Figure 11. In addition, the baseline design uses 4 Minco model S665 thermal

tab sensors per grating module, for a total of 120 sensors in the grating array. Using 4 heaters and 4 temperature sensors at each module will provide redundancy while detecting and correcting any gradients in the module. Given the large number of heaters and sensors a trade study will be performed to see if control could be done at the grating array platform insert or at the platform assembly level. The exact configuration will be determined during the design phase. Given the above reference design, the power requirements for the OP-XGS grating thermal control are given in Table 3.

Thermal Control Unit	Nominal Power (W)	Maximum Power (W)
Command and Telemetry	1	2
Power Converter	1	5
Power Distribution Assembly	1	2
Minco Heater (120)	10	120
Minco Sensors (120)	1	5
Total	14	134

Table 3: OP-XGS grating array thermal control power budget.

3. SUMMARY

We have presented here a mature design for an OP-XGS that will meet the soft X-ray throughput and spectral resolution requirements for *IXO*. This design utilizes 540 co-aligned reflection gratings in the extreme off-plane mount. This array of gratings is contained within a monolithic structure that mounts to the spacecraft avionics bus module located 13.5 m away from the focal plane. This layout combined with the dispersion of the gratings determines the size of the CCD array at the focal plane. The CCD array incorporates 9 CCDs, one for a zero order monitor and 8 to collect the spectra. These CCDs measure 15 mm x 30 mm and are capable of a 32 Hz frame rate reading from 4 output nodes per CCD. Thermal control requirements and preliminary designs based on those requirements have been developed for both the grating array and CCD array. Finally, table 4 provides a summary of the components of these arrays along with the associated mass. The design fits easily within the nominal mass envelope of 100 kg for the *IXO* XGS.

Spacecraft Bus Component	Qty.	kg per	Total kg	Instrument Module Component	Qty.	kg per	Total kg
Grating Array			44.7	CCD Camera			20.0
Array structure	1	7.0	7.0	Enclosure	1	2	2.0
Platform insert	1	12.0	12.0	Proximity electronics card	1	2.1	2.1
Module structure	30	0.3	9.9	Radiation shielding	1	8	8.0
Gratings	540	0.0	15.1	Cold finger	10	0.1	1.0
Mounting screws NAS1352	90	0.002	0.2	Thermal control card	2	0.5	1.0
Mounting nuts MS1043	90	4e-4	0.0	Radiator	1	5	5.0
Washers	90	0.006	0.5	CCDs	9	0.1	0.9
Grating Thermal Control			10.2	Drive electronics			4.2
Power converter	1	0.5	0.5	Enclosure	1	1	1.0
Command and Telemetry	1	0.5	0.5	Signal processing card	4	0.5	2.0
Minco thermofoil heaters HK5568	120	0.002	0.2	Housekeeping card	2	0.3	0.6
Minco thermal sensor S665	120	0.002	0.2	Drive thermal control card	2	0.3	0.6
Power distribution assembly	1	2.0	2.0	Digital processing electronics			2.2
Electronics box	1	2.0	2.0	Enclosure	1	1	1.0
Cable harness	480	0.01	4.8	Bus interface	1	0.3	0.3
Total			54.9	Camera Control Card	1	0.3	0.3
Total OP-XGS Mass = 81 kg Table 4:OP-XGS mass summary				Discriminator	1	0.3	0.3
				Command Card	1	0.3	0.3
				Total			26.4

REFERENCES

1. McEntaffer, R. L., Cash, W., Shipley, A., "Off-plane reflection gratings for Constellation-X" *Proc. SPIE*, 7011, 701107 (2008).
2. Osterman, S. N., McEntaffer, R. L., Cash, W., Shipley, A., "Off-plane grating performance for Constellation-X" *Proc. SPIE*, 5488, 302 (2004).
3. Cash, W. C., "X-ray optics. 2: A technique for high resolution spectroscopy," *Appl. Opt.*, 30, 1749, (1991).
4. Shipley, A., & McEntaffer, R. L., "Thin substrate grating array for sounding rocket and satellite payloads" *Proc. SPIE*, 7011, 70112I (2008).
5. den Herder, J. W., et al., "The Reflection Grating Spectrometer on board XMM-Newton," *A&A*, 365, L7 (2001).
6. Jorden, P. R., Morris, D. G., Pool, P. J., "Technology of large focal planes of CCDs," *Proc. SPIE*, 5167, 72 (2004).